Proof of a LOD prediction model with orthogonal PAT methods in continuous wet granulation and drying

Katharina Kiricenko , Stefan Klinken , Peter Kleinebudde

PII: S0022-3549(24)00254-5
DOI: https://doi.org/10.1016/j.xphs.2024.07.008
Reference: XPHS 3474

To appear in: *Journal of Pharmaceutical Sciences*

Received date: 5 April 2024
Revised date: 9 July 2024
Accepted date: 9 July 2024

Please cite this article as: Katharina Kiricenko , Stefan Klinken , Peter Kleinebudde , Proof of a LOD prediction model with orthogonal PAT methods in continuous wet granulation and drying, *Journal of Pharmaceutical Sciences* (2024), doi: https://doi.org/10.1016/j.xphs.2024.07.008

Highlights

- Implementation of an orthogonal process analytical technology approach for loss-on-drying monitoring using near-infrared spectroscopy and mass balance within a vibrated fluidized bed dryer-
- Loss-on-drying prediction model based on key process parameters was developed and verified.
- Demonstrated the feasibility of predicting a process parameter to achieve a desired moisture content.
- Low-cost, in-house built near infrared spectroscopy sensor correlated good with the measurement via mass balance.

Proof of a LOD prediction model with orthogonal PAT methods in continuous wet granulation and drying

Katharina Kiricenko[a], Stefan Klinken[a], Peter Kleinebudde[a]*

[a] Heinrich Heine University Düsseldorf, Faculty of Mathematics and Natural Science, Institute of Pharmaceutics and Biopharmaceutics, Universitätsstraße 1, 40225 Düsseldorf, Germany

* Corresponding author. E-mail address: kleinebudde@hhu.de

Abstract

Real-time monitoring of critical quality attributes, such as residual water in granules after drying which can be determined through loss-on-drying (LOD), during wet granulation and drying is essential in continuous manufacturing. Near-infrared (NIR) spectroscopy has been widely used as process analytical technology (PAT) for in-line LOD monitoring. This study aims to develop and apply a model for predicting the LOD based on process parameters. Additionally, the efficacy of an orthogonal PAT approach using NIR and mass balance (MB) for a vibrating fluidized bed dryer (VFBD) is demonstrated. An in-house-built, cost-effective NIR sensor was utilized for measurements and exhibited good correlation compared to standard method via infrared drying. The combination of NIR and MB, as independent methods, has demonstrated their applicability. A good correlation, with a Pearson r above 0.99, was observed for LOD up to 16 % (w/w). The use of an orthogonal PAT method mitigated the risk of false process adaption. In some experiments where the NIR sensor might have been covered by powder and therefore did not measure accurately, LOD monitoring via MB remained feasible. The developed model effectively predicted LOD or process parameters, resulting in an R2 of 0.882 and a RMSE of 0.475 between predicted and measured LOD using the standard method.

Keywords

Continuous manufacturing; PAT; Vibrated fluidized bed dryer; Mass balance; NIR spectroscopy; LOD prediction

Abbreviations:

AF: Inlet air flow; API: active pharmaceutical ingredient; CM: Continuous manufacturing; DoE: Design of Experiment; DT: Drying temperature; FBD: Fluidized bed dryer; IBU: Ibuprofen; IR: Infrared; KE: Kneading

element; L/S: Liquid-to-solid ratio; LOD: loss-on-drying; LPCE: Long pitch conveying element; MB: Mass balance; MCC: Microcrystalline cellulose; MCCV: Monte-Carlo cross-validation; NIR: Near-infrared; PAT: Process analytical technology; PVP: Polyvinylpyrrolidone; RMSE: Root mean square error; RMSECV: Root mean square error of cross validation; SFR: Solid feed rate; SPCE: Short pitch conveying element; TSG: Twin-screw wet granulation; VFBD: Vibrated fluidized bed dryer; Vib: Vibration acceleration

1. Introduction

Continuous wet granulation and drying processes represent a fundamental opportunity in the production of solid dosage forms, offering numerous advantages over traditional batch production. These advantages include lower waste and constant product quality due to less variabilities within the product.[1] Twin-screw wet granulation (TSG) is a favorable process choice in continuous granulation. Several types of dryers have been investigated in the literature for implementation in continuous manufacturing (CM) lines. Among those are segmented fluid bed dryer (FBD)[2-4], horizontal FBD with a screw conveyer[5] or vibrated fluidized bed dryer (VFBD)[6-8]. Granule size distribution[9], flow properties, porosity and moisture content[10] of the final granules might influence the product quality, independent whether the granules are further processed into tablets or not. To ensure consistent product quality an adequate control system for these is necessary.

Therefore, the U.S. Food and Drug Administration FDA encourage the implementation of process analytical technologies (PATs) to improve manufacturing processes. These PAT systems enhance process understanding, facilitate continuous improvement and support risk-mitigation strategies.[11] There are several PATs available to monitor one of the most important critical quality attributes during granulation and drying, the water content, which can be determined as loss-on-drying (LOD). The amount of residual water in the granules after drying is defined as LOD. One commonly PAT method is near infrared (NIR) spectroscopy, which has been extensively investigated in the literature.[2, 10, 12-17] The use of microwave resonance technology offers an alternative approach for PAT.[15, 18, 19] Both methods providing a fast and non-destructive technique.[12, 13, 15, 18] Nevertheless, multivariate analysis, such as partial least square regression[12, 20] or multiple linear regression[15, 21], are required for calibration to predict the water content using a reference method e.g. Karl Fisher titration or moisture analyzer using infrared (IR) light as heat source to determine LOD.[12, 20, 22] Microwave resonance technology was implemented in a FBD as a PAT method for LOD monitoring.[15, 19, 21]

Mathematical models and numerical simulations are used more frequently in the literature today to predict the LOD.[23-25] Soft sensor[26, 27] and data-driven technique using latent-variable model with

knowledge-driven mechanic model were implemented for segmented-FBD[27-29] and VFBD[7, 30, 31]. The LOD can be predicted based on the installed sensors using mass balance (MB) in real time. This approach has been previously introduced for segmented-FBD[2, 20] and VFBD[32]. A notable benefit is that no additional sensors need to be purchased or installed, allowing direct calculation without the need for calibration and irrespective of the material being processed.[2, 32] The combination of MB, another soft sensor or mathematical models with a standard PAT approach, such as microwave resonance or NIR spectroscopy, enables orthogonal and independent process control, thereby reducing the risk of erroneous control decisions in case of issues with the PAT. This approach is well described in literature. For instance, Pauli et al. implemented an orthogonal redundant method for a segmented-FBD.[2]

The aim of the study was to develop a model predicting the LOD based on process parameters, and further, to determine the necessary settings for one process parameter to achieve a specific LOD value, measured through loss-on-drying using IR, NIR spectroscopy, and predicted with MB. Additionally, the study aims to explore the application of a low-cost NIR sensor alongside MB prediction as an orthogonal and redundant PAT method.

2. Materials and methods

2.1. Materials

Two mixtures consisting of alpha-lactose monohydrate (GranuLac® 200, MEGGLE, Wasserburg am Inn, Germany) and microcrystalline cellulose (MCC, VIVAPUR® 101, JRS PHARMA, Rosenberg, Germany) were selected as model formulations based on previous studies.[6, 32] MCC is an important excipient used in the manufacturing of solid oral dosage forms and the water absorption capacity of MCC makes the formulations more challenging during drying. Polyvinylpyrrolidone K 30 (PVP, Kollidon® 30, BASF SE, Ludwigshafen, Germany) was used as binder. Further formulations were investigated containing Ibuprofen (IBU, Ibuprofen 50, BASF SE, Ludwigshafen, Germany) as an active pharmaceutical ingredient (API). Two different levels for the drug content were utilized together with alpha-lactose monohydrate and MCC. In total, four formulations were investigated in this study as described in Table 1. This allows the application of different formulation and enables the analysis of whether the methods and models for LOD are applicable. The physical characterization of the mixtures regarding particle size distribution, flowability and initial LOD is provided in the supplement

(Supplement Table 1). IBU was deagglomerated before mixing using a high-speed conical mill (BTS100, L.B. Bohle Maschinen und Verfahren, Ennigerloh, Germany) with a sieve mesh of 1.0 mm. Each powder mixture was blended for 20 min at 25 rpm in a lab-scale blender (LM 40, L.B. Bohle Maschinen und Verfahren, Ennigerloh, Germany). Demineralized water was utilized as granulation liquid during TSG.

2.2. Methods

2.2.1. Model development using DoE

Wet granulation and drying were executed using the QbCon® 1 (L.B. Bohle Maschinen und Verfahren, Ennigerloh, Germany) which consist of a 16 mm twin-screw granulator and a vibrated fluidized bed dryer. The CM line has been described in previous studies[6, 32] and was used by other researchers.[8, 30, 33, 34] The screw configuration for all experiments included long pitch conveying elements (LPCE), short pitch conveying elements (SPCE) and kneading elements (KE) with a stagger angle of 60°. Screw configuration was as follows in flow direction: 4D LPCE – 3.75D SPCE – 1.2D (6) KE – 5D SPCE – 1.2D (6) KE – 5D SPCE. The powder was fed using a gravimetric feeder (DIW-PE-GZD-P 150.12 Gericke AG, Regensdorf, Switzerland). Granulation liquid was added before the first kneading block using a micro-gear pump (MZR-7205, HNO-Mikrosysteme GmbH, Schwerin, Germany) with a nozzle diameter of 0.12 mm.

The LOD prediction model was developed by performing a D-optimal Design of Experiment (DoE) using the 17 % MCC formulation. The solid feed rate (SFR), liquid-to-solid ratio (L/S), drying temperature (DT), inlet air flow (AF) and vibration acceleration (Vib) were investigated as factors. The factor ranges used were 1 – 2 kg/h for SFR, 15 – 25 % for L/S ratio, 40 – 80 °C for DT, 10 – 20 Nm^3/h for AF and 4 8 m/s^2 for Vib. The D-optimal design was created using the software MODDE (V13.0, Sartorius Stedim Data Analytics AV, Malmö, Sweden). The DoE initially consisted of 28 runs and was complemented with additional runs, resulting in a total of 40 runs, including a fivefold center point. To build the setup of the DoE, 21 model terms were selected to be included in the design (SFR; L/S; DT; AF; Vib; DT*DT; AF*AF; Vib*Vib; SFR*SFR; L/S*L/S; DT*AF; DT*Vib; DT*SFR; DT*L/S; AF*Vib; AF*SFR; AF*L/S: Vib*SFR; Vib*L/S; SFR*L/S and the constant). All runs were performed in a randomized order and analyzed with the software MODDE. The optimization of the models involved

backward regression by excluding non-significant effects based on their p-value, starting with the highest value. Runs were excluded if they deviated from the normal residual distribution, defined as being beyond 3 standard deviations. Thus, the obtained models were not suitable to describe the excluded runs. For the IR model, run 4 was excluded. For the NIR model, a total of five runs were excluded (Runs 4, 17, 27, 33 and 35). The dryer was preheated for 30 min at the beginning of each day. Each run included a 15 min equilibration period to adjust for changes in factors, followed by 45 min processing time with sampling conducted every 5 min for the LOD determination. In total, 60 kg of material was used to conduct the DoE. LOD was determined using the offline method via moisture analyzer, inline using NIR spectroscopy and predicted by applying the mass balance.

2.2.2. Model verification

For the verification of the developed model additional runs were performed as listed in Table 3. Runs A - O were conducted to adjust one process parameter while keeping the others constant to achieve a target LOD using the 17 % MCC formulation. The variation of these individual parameters was calculated or predicted by rearranging the LOD model obtained from IR to one of the process parameters. The runs P - T were executed with each of the four formulations (17 %, 34 % MCC, 20 % IBU or 67 % IBU).

2.2.3. Determination of LOD via moisture analyzer

During the drying process, granules were sampled every 5 min at the outlet and the LOD was determined by measuring the moisture driven-off offline using the moisture analyzer (MA 100, Sartorius, Goettingen, Germany). IR light was used for heating of the sample. For collecting granules, a snap glass was held at the outlet of the dispersion unit and the entire sample was collected for approximately 30 s. The sample size was approximately 2 g. 17 % MCC and 34 % MCC formulation were dried at 80 °C and 20 % IBU and 67 % IBU formulation at 60 °C. The endpoint of the measurement was set to 0.1 % mass variation over 150 s.

2.2.4. Prediction of LOD via mass balance

During the granulation and drying processes, process parameters were recorded by the installed sensors of the machine. This includes SFR and liquid feed rate for the TSG. Additionally, during the drying phase, parameters such as air flow, temperature, humidity and pressure of both the inlet and outlet air were continuously monitored and utilized for mass balance calculations. The data were

collected with a sample frequency of 1 Hz. The ambient air was also included into the MB therefore the air pressure was measured. Temperature and humidity were noticed every 30 min using the wireless temperature and humidity sensor testo 175 H1 (Testo SE, Titisee-Neustadt, Germany). The difference between the amount of water entering and leaving the dryer in empty state was detected. Thus, a correction factor was implemented based on the difference of water recorded in empty state. The stepwise deviation of the MB was applied in accordance to a previous study[32].

2.2.5. In-line LOD determination via NIR spectroscopy

The in-line measurement of the LOD using NIR spectroscopy (Raspberry spegg® NIR22, Dr. Licht, Nümbrecht, Germany) was conducted with a low-cost, in-house-built NIR sensor. A LED light source with a peak frequency of 1450 nm was coupled to a hexa-core optical fiber. The light source was powered with a current of around 100 mA. The current was slightly adjusted in the experiments to ensure a sufficient illumination of the granules under various process setting and to avoid clipping of the spectra. The full price of the NIR measurement system was around 3600 €. The spectra were recorded in reflection at a frequency of 0.5 Hz. The spectral range was between 1000 and 1750 nm with a resolution expressed as the full width half maximum of below 16 nm. The spectra were filtered using a moving average filter in a width of 3 values of the wavelength. The sampling time points for the LOD measurements were manually recorded, and the arithmetic mean of the spectra at these time points $\pm$ 30 s were used as the calibration set for the model described below. Subsequently after mean-centering maximum scaling of the spectra, the range between 1300 and 1600 nm was correlated with the offline measured LOD values using a PLS1. The raw and pretreated spectra are shown in the supplement (Fig S1). The mean squared error of a Monte-Carlo-cross-validation (MCCV) was used to optimize the number of latent structures. The validation split procedure was repeated 1000 times with 80 % of the data in training data set. The experimental setup is given in Figure 1. Dried granules leave the dryer through the rotary valve. A vibratory dispersion unit is positioned beneath the outlet to create a thin granule bed with an approximate linear velocity of 0.0073 m/s, improving the measurements via NIR probe. The granules were sampled after passing the dispersion unit and NIR probe for offline measurements, as described in section *2.2.3. Determination of LOD via moisture analyzer.* Therefore, all granules that passed the NIR probe were also sampled LOD measurements using moisture analyzer.

3. Results and discussion

3.1. NIR spectroscopy calibration

For the construction of the NIR model 13 latent structures were found to be most suitable based on the cross-validation procedure. Figure 2 displays the correlation between the measured LOD via IR and the predicted LOD via NIR, including the prediction of the MCCV. The low-cost sensor showed good agreement between the predicted and measured LOD, with a R^2_{MCCV} of 0.91. The root mean square error of the MCCV (RMSECV) was determined to be 1.24 %. Some data points, e.g. predicted LOD between 6 to 10 %, exhibited greater deviation from the line of identity. Additionally, there were consecutive runs in the DoE that deviated from the measured LOD via IR and LOD via MB. It seems that the NIR sensor was covered by fine powder and thus unable to measure accurately. Nevertheless, the low-cost NIR sensor is suitable for predicting LOD within a range between 0 to 20 %. It should be noted that the accuracy of the NIR is higher at lower LOD values, as the granules become drier and more uniform. At higher LOD values, there may be large granules of higher residual water and fine granules of low residual water after drying. Such uneven distribution reduces the accuracy.

3.2. LOD prediction model

3.2.1. Model evaluation

The LOD was measured and determined using the IR, NIR and MB approaches. Therefore, three individual models were built based on the LOD determination approach. Since the NIR method is calibrated against the IR method, NIR should be considered together with the IR. Figure 3 illustrates the evaluation of the model for predicting the logarithmic LOD. LOD was logarithmically transformed to ensure a normal distribution of the data. In the IR model (Fig 3A) one run was excluded. In the NIR (Fig 3B), five runs were excluded, while using the LOD model via MB (Fig 3C), all runs were included. The reason for excluding runs is described in the section *2.2.1. Model development using DoE.* All models displayed high values for the measure of fit, R^2 (> 0.90) and the predictability Q^2 resulted in > 0.97, except for Q^2 (MB), which was 0.87. Comparing the coefficient plots of all three models, more factors and interactions are included in the models for LOD measured via IR and NIR. However, in the model set up with LOD via MB only the main factors are involved. Except for MB model (-0.2), the models demonstrated sufficient model validity (> 0.25), indicating no lack of fit. In case of MB, the model error is significantly larger than the pure error (reproducibility) according to MODDE.[35] The

models without excluding runs for IR and NIR models are attached in the supplementary (supplement Fig 2). Thereby, less coefficients are involved in the models and a model validity below 0.25 is obtained. The exclusion of data points that were not properly described by the model led to more coefficients being included in the model and improved R^2, Q^2 and model validity. The comparison of the coefficients showed that if the same coefficients were included, the influence on the LOD of the factors and factor combinations on the LOD consistent. By increasing the DT or AF, the LOD decreased as more water was removed from the granules. Increasing the Vib reduced the residence time of the granules inside the drying chamber, exposing the granules to hot and dry air for a shorter duration, which led to an increased LOD. An increased LOD was also obtained by increasing the SFR, as this led to a larger granules bed inside the chamber and thus less efficient drying. Additionally, with an increased L/S ratio, the LOD increased. The impact of the drying parameters corresponds to the findings from the previous study where a central composite design was used.[7]

3.2.2. Application

The developed models to predict the LOD were verified using additional 16 runs (A-O), whereby run B was conducted twice as an error was assumed. The predicted LOD values based on the applied process parameter are plotted against the LOD measured offline with IR (Fig 4). The best agreement between predicted and observed data was found for the IR model (Fig 4A) followed by the NIR model (Fig 4C). The NIR should not deviate substantially from IR, as the calibration is based on these values, and this method cannot be considered independent. This resulted in a R^2 of 0.882 and a RMSE of 0.475 using the IR model, and a R^2 of 0.866 and RMSE of 0.756 predicted with the NIR model. All LOD values, independent of the model, were overpredicting below 3 %. A larger scattering of the LOD above the line of identity was obtained for the model built via NIR (Fig 4C), resulting in a larger RMSE for NIR compared to the other two models. The reason might be the inaccurate measuring of the NIR sensor due to the covering of the sensor with powder, which was mentioned in the section *3.1. NIR spectroscopy calibration.* These runs are nevertheless included in the model and thus led to an error in the prediction. The MB model yielded a R^2 of 0.847 and a RMSE of 0.541. The MB model showed underprediction at LOD values above 3 % and overprediction below 3 %. By considering the error bars, which represent the prediction interval at a confidence level of 95 %, the prediction interval of the MB model is approximately doubled compared to IR and NIR. This is due to the exclusion of runs in

case of IR and NIR, which resulted in narrow prediction intervals as the model described and predicted the LOD more accurately. In case of the MB model, all runs were included in the model, and after model optimization, the MB model is built only from the main factors and the constant, without interaction and quadratic effects as in the other two models.

In addition to these 16 runs, further runs using different formulations were investigated (P-T, Table 3). Run R was a center point from another experimental series and was therefore conducted three times. These runs were inserted into the models to predict the LOD based on the IR and MB model. The verification using different formulations is shown in Figure 5. Regardless of the formulation, both models overpredicted the LOD between 1 – 3 % LOD. The highest deviation was observed for the run T2 (Table 3) using 34 % MCC, applying a high SFR and L/S, resulting in higher water uptake of the granules and thus not sufficiently drying under the used drying conditions. At the other granulation parameters (34 % MCC formulation), the predicted and observed LODs overlapped well compared to the formulations with API. The additional runs resulted in a R^2 of 0.826 and a RMSE of 0.715 using the IR model and a R^2 of 0.768 and a RMSE of 0.829 for the MB model. As mentioned previously, the MB model consisted of larger confidence intervals for the prediction.

The development model could also predict one of the involved process parameters by keeping the others constant to achieve a target LOD. The LOD for three runs is illustrated in Figure 6. To obtain a target LOD of 2.0 % by adjusting the DT and leaving other parameters at the center point conditions, the IR model predicted a DT of 81 °C. For this the model obtained with IR from Figure 3A was used and in this case rearranged to DT. The predicted and observed LOD values for run A – O is listed in Table 4. The comparison of the observed LOD values showed good agreement between IR and NIR measurements, as well as with MB measurements. The highest deviation between observed LOD via IR and MB was determined for run L with 0.68 %. In case of IR and NIR measurements, the highest deviation was found for run M with a difference of 1.09 %.

The observed LOD measured via IR is scattered around the lower prediction limit of 1.5 % (Fig 6A). The LOD via NIR and MB is scattered below the lower limit similarly. Around 12 min, the LOD predicted via MB is increased sharply to 5.4 % and then decreased back to around 1.0 %. When comparing the raw data used for LOD prediction via MB, the SFR exhibits a temporary increase, which was also reflected in the prediction (Fig 6B). This demonstrates how sensitive the process control via MB is. Any changes in the process parameter affecting the LOD are directly observed. To reach a

LOD of 0.95 % by adjusting the AF while keeping the drying conditions as in run D (Fig 6A), the IR model calculated an AF of 19.9 Nm3/h. The observed LODs showed a scattering among all three methods around the target LOD and lower prediction limit (Fig 6C). In run D, the LOD was adjusted to 2.7 % by changing the L/S ratio from 0.20 to 0.238. The observed LOD values scattered between target and upper prediction limits (Fig 6D).

In total, 84 runs were conducted including various formulations. To assess the suitability of the MB and NIR spectroscopy methods, the average deviation to the standard method was calculated. The absolute average deviation, also referred to as bias, between MB and standard LOD method was determined to be 0.23 %, while that between NIR and standard approach was 0.37 %. The maximal individual absolute deviation was found to be 0.81 % for MB and 3.63 % for NIR. The average absolute deviation between MB and NIR was calculated to be 0.47 %. By comparing these results to the reported by Pauli et al., similar absolute LOD deviations were observed.[2]

The comparison between the LOD measured via MB and NIR for all conducted runs is displayed in Figure 7. The correlation between both methods resulted in a Pearson r of 0.952 and a RMSE of 0.760 (Fig 7A). The red points showed large deviations between the LOD predicted via NIR and MB. However, the LOD via MB and the standard method IR showed similar values. As mentioned before, in some runs of the DoE in series, the NIR sensor might have been covered by powder. This demonstrated that if the process control via NIR shows high deviation in the critical quality attribute, it requires a process adaptation. By comparing the LOD values observed with MB, which is independent of NIR, LOD values might be within the acceptance limits. Thus, the MB method could monitor the LOD additionally to reduce the risk of correcting the process based on the wrong signal. By removing these deviated runs, a good agreement with a r of 0.996 and RMSE of 0.433 were obtained (Fig 7B). This showed that the MB and NIR methods in combination formed an orthogonal PAT method, allowing independent process control of the LOD. Therefore, if the PAT method e.g. NIR spectroscopy shows values which requires a process adaptation, the second method helps to decide if there is a measurement error or indeed a deviation in the process. The low-cost NIR sensor was able to predict the LOD appropriately.

4. Conclusion

In this study, a LOD prediction model was developed to predict the LOD either by applying various process parameters involved in continuous wet granulation and VFBD or by determine an individual process parameter required to achieve a target LOD. The LOD was successfully measured using the offline IR method along with MB and NIR spectroscopy. The developed prediction models, particularly those using IR and MB for LOD determination, exhibited reliable prediction for LODs up to 5 %. Since the developed model was not able to describe all 40 runs based on the residual standard deviation, some runs were excluded. In the case of the MB model, all runs were included to develop the model. This led to a reduction in prediction accuracy as larger prediction intervals were obtained. The built MB model involved only the main factors, whereas the other two models also included interactions and quadratic effects. The in-house built NIR sensor, calibrated offline with IR, demonstrated accurate LOD prediction. However, it was observed that the sensor was more prone to errors due to its installed position at the outlet, which resulted in it being covered by powder. Consequently, frequent cleaning of the sensor might be necessary for obtaining reliable LOD values throughout the entire process. Therefore, compressed air might be useful to dedust the sensor at defined time intervals. The applied MB for the LOD determination, based on logged sensor data measuring AF, humidity, temperature and pressure of incoming and exiting air, provided a cost-effective alternative to standard PAT methods such as microwave resonance or NIR spectroscopy. As these methods require an initial cost implementation and involve time-consuming calibration and validation processes, which included an additional reference method. It needs to be considered that the MB predicts more reliably if the drying process is in steady-state conditions as demonstrated in a previous study.[32] Small deviations in the involved process parameters might predict a higher or lower LOD, which is not realistic, as the MB is too sensitive. This sensitivity of the MB prediction must be considered with caution, as it is unclear how the fluctuation of a process parameter, e.g. powder feed rate, is dampened and whether the LOD is affected. The sample frequency of 5 min was too low to provide information in this case. The application of MB and NIR spectroscopy, which independently determined the LOD, showed good agreement in LOD values up to 16 %. Utilizing two independent methods reduces the risk of making false process adaption based solely on PAT signals. This study demonstrated the two independent models (IR and MB) capable of predicting LOD based on the involved process parameters, or inversely, calculating a process parameter to achieve a certain LOD. Additionally, it highlights the importance of orthogonal PAT methods and verifies the applicability of the MB model, in combination with NIR spectroscopy, for LOD monitoring during drying via VFBD.

Acknowledgements

The authors thank Dr. Robin Meier, Andreas Altmeyer and Daniel Emanuele for their constructive feedback and insightful discussion throughout the derivation of mass and energy balance. A thank to Meggle for providing GranuLac® 200 and BASF SE for Kollidon® 30. Additionally, thanks to Martin Lück for his support during the conduction of the experiments and feedback on an earlier version of the manuscript.

Declaration of interest

None

Funding sources

Stefan Klinken was supported by the German Research Foundation (DFG). SPP 2364, Grant number: 504702251.

Data availability

The data are available on request.

Appendix A. Supplementary Material

Supplementary data to this article can be found online at xxxxxxxxxxxxx.

References

1. Plumb K. Continuous processing in the pharmaceutical industry. Chem Eng Res Des 2005;83(6):730-738. https://doi.org/10.1205/cherd.04359.

2.Pauli V, Elbaz F, Kleinebudde P, et al. Orthogonal redundant monitoring of a new continuous fluid-bed dryer for pharmaceutical processing by means of mass and energy balance Calculations and Spectroscopic Techniques. J Pharm Sci 2019;108(6):2041-2055. https://doi.org/https://doi.org/10.1016/j.xphs.2018.12.028.

3.Monaco D, Omar C, Reynolds GK, et al. Drying in a continuous wet granulation line: Investigation of different end of drying control methods. Powder Technol 2021;392:157-166. https://doi.org/10.1016/j.powtec.2021.07.004.

4.Vercruysse J, Peeters E, Fonteyne M, et al. Use of a continuous twin screw granulation and drying system during formulation development and process optimization. Eur J Pharm Biopharm 2015;89:239-247. https://doi.org/10.1016/j.ejpb.2014.12.017.

5.Zhang YW, Abatzoglou N, Hudon S, et al. Dynamics of heat-sensitive pharmaceutical granules dried in a horizontal fluidized bed combined with a screw conveyor. Chem Eng Process 2021;167. https://doi.org/https://doi.org/10.1016/j.cep.2021.108516.

6.Kiricenko K, Kleinebudde P. Drying behavior of a horizontal vibrated fluidized bed dryer for continuous manufacturing. Pharm Dev Technol 2023;28(5):440-451. https://doi.org/10.1080/10837450.2023.2205932.

7.Wikstrom H, Martin de Juan L, Remmelgas J, et al. Drying capacity of a continuous vibrated fluid bed dryer - Statistical and mechanistic model development. Int J Pharm 2023;645:123368. https://doi.org/10.1016/j.ijpharm.2023.123368.

8.Franke M, Riedel T, Meier R, et al. Scale-up in twin-screw wet granulation: impact of formulation properties. Pharml Dev Technol 2023:1-14. https://doi.org/10.1080/10837450.2023.2276791.

9.Pauli V, Roggo Y, Kleinebudde P, et al. Real-time monitoring of particle size distribution in a continuous granulation and drying process by near infrared spectroscopy. Eur J Pharm Biopharm 2019;141:90-99. https://doi.org/https://doi.org/10.1016/j.ejpb.2019.05.007.

10.Fonteyne M, Vercruysse J, Diaz DC, et al. Real-time assessment of critical quality attributes of a continuous granulation process. Pharm Dev Technol 2013;18(1):85-97. https://doi.org/10.3109/10837450.2011.627869.

11.U.S. Department of Health and Human Services Food and Drug Administration. Guidance for Industry: PAT - A Framework for Innovative Pharmaceutical Development, Manufacturing, and Quality Assurance. FDA; 2004.

12.Chablani L, Taylor MK, Mehrotra A, et al. Inline real-time near-infrared granule moisture measurements of a continuous granulation-drying-milling process. AAPS PharmSciTech 2011;12(4):1050-1055. https://doi.org/10.1208/s12249-011-9669-z.

13.Fonteyne M, Arruabarrena J, de Beer J, et al. NIR spectroscopic method for the in-line moisture assessment during drying in a six-segmented fluid bed dryer of a continuous tablet production line: Validation of quantifying abilities and uncertainty assessment. J Pharm Biomed Anal 2014;100:21-27. https://doi.org/https://doi.org/10.1016/j.jpba.2014.07.012.

14.Fonteyne M, Soares S, Vercruysse J, et al. Prediction of quality attributes of continuously produced granules using complementary pat tools. Eur J Pharm Biopharm 2012;82(2):429-436. https://doi.org/https://doi.org/10.1016/j.ejpb.2012.07.017.

15.Peters J, Teske A, Taute W, et al. Real-time process monitoring in a semi-continuous fluid-bed dryer – microwave resonance technology versus near-infrared spectroscopy. Int J Pharm 2018;537(1):193-201. https://doi.org/https://doi.org/10.1016/j.ijpharm.2017.12.040.

16.Mu G, Liu T, Liu J, et al. Calibration model building for online monitoring of the granule moisture content during fluidized bed drying by NIR spectroscopy. Ind Eng Chem Res 2019;58(16):6476-6485. https://doi.org/10.1021/acs.iecr.8b05043.

17.Domokos A, Pusztai É, Madarász L, et al. Combination of PAT and mechanistic modeling tools in a fully continuous powder to granule line: Rapid and deep process understanding. Powder Technol 2021;388:70-81. https://doi.org/10.1016/j.powtec.2021.04.059.

18.Buschmuller C, Wiedey W, Doscher C, et al. In-line monitoring of granule moisture in fluidized-bed dryers using microwave resonance technology. Eur J Pharm Biopharm 2008;69(1):380-387. https://doi.org/10.1016/j.ejpb.2007.09.014.

19.Peters J, Taute W, Bartscher K, et al. Design, development and method validation of a novel multi-resonance microwave sensor for moisture measurement. Anal Chim Acta 2017;961:119-127. https://doi.org/10.1016/j.aca.2017.01.021.

20.Fonteyne M, Gildemyn D, Peeters E, et al. Moisture and drug solid-state monitoring during a continuous drying process using empirical and mass balance models. Eur J Pharm Biopharm 2014;87(3):616-628. https://doi.org/10.1016/j.ejpb.2014.02.015.

21.Peters J, Bartscher K, Doscher C, et al. In-line moisture monitoring in fluidized bed granulation using a novel multi-resonance microwave sensor. Talanta 2017;170:369-376. https://doi.org/10.1016/j.talanta.2017.03.105.

22.Peters J, Teske A, Taute W, et al. Real-time process monitoring in a semi-continuous fluid-bed dryer - microwave resonance technology versus near-infrared spectroscopy. Int J Pharm 2018;537(1-2):193-201. https://doi.org/10.1016/j.ijpharm.2017.12.040.

23.Temple SJ, van Boxtel AJB. Modelling of fluidized-bed drying of black tea. J Agric Eng Res 1999;74(2):203-212. https://doi.org/10.1006/jaer.1999.0454.

24.Picado A, Martínez J. Mathematical Modeling of a Continuous Vibrating Fluidized Bed Dryer for Grain. Drying Technol 2012;30(13):1469-1481. https://doi.org/10.1080/07373937.2012.690123.

25.Zhang Y, Abatzoglou N. Modelling of continuous drying of heat-sensitive pharmaceutical granules in a horizontal fluidised bed dryer combined with a screw conveyor at steady state. Chem Eng Sci 2022;255. https://doi.org/10.1016/j.ces.2022.117678.

26.Lu M, Kranz P, Salmon A, Wilkinson S, et al. Heat transfer model and soft sensing for segmented fluidized bed dryer. Processes 2022;10(12). https://doi.org/10.3390/pr10122609.

27.Rehrl J, Sacher S, Horn M, et al. End-Point prediction of granule moisture in a ConsiGma-25 segmented fluid bed dryer. Pharmaceutics 2020;12(5). https://doi.org/10.3390/pharmaceutics12050452.

28.Destro F, Salmon AJ, Facco P, et al. Monitoring a segmented fluid bed dryer by hybrid data-driven/knowledge-driven modeling. IFAC-PapersOnLine 2020;53(2):11638-11643. https://doi.org/10.1016/j.ifacol.2020.12.646.

29.Ghijs M, Schäfer E, Kumar A, et al. Modeling of semicontinuous fluid bed drying of pharmaceutical granules with respect to granule size. J Pharm Sci 2019;108(6):2094-2101. https://doi.org/https://doi.org/10.1016/j.xphs.2019.01.013.

30.E Elkhashap A, Meier R, Abel D. Modeling and control of a continuous vibrated fluidized bed dryer in pharmaceutical tablets production. Pharm Ind 2019;81(12):1693-1700.

31.Lehmann SE, Buchholz M, Jongsma A, et al. Modeling and flowsheet simulation of vibrated fluidized bed dryers. Processes 2020;9(1). https://doi.org/10.3390/pr9010052.

32.Kiricenko K, Hartmann F, Altmeyer A, et al. Loss-on-drying prediction for a vibrated fluidised bed dryer by means of mass and energy balances. J Pharm Innov 2023;18(4):2429-2446. https://doi.org/10.1007/s12247-023-09802-w.

33.Franke M, Riedel T, Meier R, et al. Comparison of scale-up strategies in twin-screw wet granulation. Int J Pharm 2023;641:123052. https://doi.org/10.1016/j.ijpharm.2023.123052.

34.Meier R, Emanuele D, Harbaum P. Important elements in continuous granule drying processes. TechnoPharm 2020;10(2):92-101.

35. Sartorius Stedim Data Analytics AB. MODDE 12 User Guide. Available at: https://www.sartorius.com/download/544636/modde-12-user-guide-en-b-00090-sartorius-data.pdf. Accessed 11.03.2024.

Tables

Table 1. Composition of the four different formulations.

Formulation name	Amount (w/w) / %			
	IBU	Lactose	MCC 101	PVP K30
17 % MCC	-	80	17	3
34 % MCC	-	63	34	3
20 % IBU	20	60	17	3
67 % IBU	67	13	17	3

Table 2. D-optimal DoE setup.

Run order	Factors				
	SFR / kg/h	L/S / -	DT / °C	AF / Nm^3/h	Vib / m/s^2
1	2.00	0.20	60.0	15.0	6.0
2	1.50	0.20	60.0	15.0	6.0
3	1.00	0.15	80.0	10.0	8.0
4	1.00	0.15	80.0	20.0	5.3
5	1.50	0.25	60.0	15.0	6.0
6	1.00	0.25	40.0	20.0	4.0
7	2.00	0.15	80.0	20.0	8.0
8	2.00	0.15	80.0	10.0	4.0
9	1.33	0.15	80.0	20.0	4.0
10	1.00	0.25	80.0	20.0	8.0
11	1.00	0.15	40.0	20.0	8.0
12	1.00	0.15	80.0	13.3	4.0
13	2.00	0.15	40.0	10.0	8.0
14	1.50	0.20	60.0	15.0	6.0
15	1.50	0.20	60.0	10.0	6.0
16	2.00	0.15	40.0	20.0	4.0
17	1.00	0.22	80.0	20.0	4.0
18	2.00	0.25	40.0	10.0	4.5
19	1.50	0.20	60.0	15.0	6.0
20	1.50	0.20	40.0	15.0	6.0
21	2.00	0.25	40.0	20.0	8.0
22	1.00	0.25	80.0	10.0	4.0
23	2.00	0.25	80.0	20.0	4.0
24	2.00	0.25	80.0	10.0	8.0
25	1.00	0.15	40.0	10.0	4.0
26	1.00	0.25	40.0	10.0	8.0
27	1.00	0.15	53.3	20.0	4.0
28	1.50	0.20	60.0	15.0	6.0
29	2.00	0.25	40.0	10.0	6.7
30	1.50	0.20	60.0	15.0	6.0
31	1.00	0.18	40.0	20.0	8.0
32	1.67	0.25	40.0	10.0	4.0
33	1.00	0.15	80.0	16.7	8.0

34	1.67	0.15	40.0	10.0	8.0
35	1.00	0.25	66.7	10.0	8.0
36	1.00	0.15	40.0	10.0	6.7
37	2.00	0.25	66.7	20.0	4.0
38	2.00	0.15	40.0	20.0	5.3
39	2.00	0.22	80.0	20.0	8.0
40	2.00	0.18	40.0	10.0	4.0

Table 3. Process parameters of the additional experiments for the model verification.

Run	Formulation				Factors				
	17 % MCC	34 % MCC	20 % IBU	67 % IBU	SFR / kg/h	L/S / -	DT / °C	AF / Nm^3/h	Vib / m/s^2
A	X	-	-	-	1.50	0.200	60.0	15.0	6.0
B	X	-	-	-	1.50	0.200	60.0	15.0	4.3
C	X	-	-	-	1.50	0.143	60.0	15.0	4.3
D	X	-	-	-	1.50	0.200	81.0	15.0	6.0
E	X	-	-	-	1.50	0.200	81.0	19.9	6.0
F	X	-	-	-	1.50	0.200	81.0	19.9	7.5
G	X	-	-	-	1.91	0.200	81.0	19.9	7.5
H	X	-	-	-	1.91	0.238	81.0	19.9	7.5
I	X	-	-	-	1.50	0.200	67.9	15.0	6.0
J	X	-	-	-	1.50	0.200	67.9	18.8	6.0
K	X	-	-	-	1.50	0.200	67.9	18.8	4.4
L	X	-	-	-	1.91	0.200	67.9	18.8	4.4
M	X	-	-	-	1.91	0.254	67.9	18.8	4.4
N	X	-	-	-	1.50	0.200	60.0	15.0	8.2
O	X	-	-	-	1.01	0.200	60.0	15.0	8.0
P1	X	-	-	-	1.00	0.150	60.0	20.0	4.0
P2	-	X	-	-	1.00	0.150	60.0	20.0	4.0
P3	-	-	X	-	1.00	0.150	60.0	20.0	4.0
P4	-	-	-	X	1.00	0.150	60.0	20.0	4.0
Q1	X	-	-	-	1.00	0.250	60.0	20.0	4.0
Q2	-	X	-	-	1.00	0.250	60.0	20.0	4.0
Q3	-	-	X	-	1.00	0.250	60.0	20.0	4.0
Q4	-	-	-	X	1.00	0.250	60.0	20.0	4.0
R1	X	-	-	-	1.50	0.200	60.0	20.0	4.0
R2	-	X	-	-	1.50	0.200	60.0	20.0	4.0
R3	-	-	X	-	1.50	0.200	60.0	20.0	4.0
R4	-	-	-	X	1.50	0.200	60.0	20.0	4.0
S1	X	-	-	-	2.00	0.150	60.0	20.0	4.0
S2	-	X	-	-	2.00	0.150	60.0	20.0	4.0
S3	-	-	X	-	2.00	0.150	60.0	20.0	4.0
S4	-	-	-	X	2.00	0.150	60.0	20.0	4.0
T1	X	-	-	-	2.00	0.250	60.0	20.0	4.0
T2	-	X	-	-	2.00	0.250	60.0	20.0	4.0
T3	-	-	X	-	2.00	0.250	60.0	20.0	4.0
T4	-	-	-	X	2.00	0.250	60.0	20.0	4.0

Table 4. Predicted LOD with 95 % confidence interval and observed LODs via IR, NIR and MB. Observed values with n = 9 (IR); n = 1350 (NIR); n = 2700 (MB), $\bar{x} \pm s$.

Run	Prediction – IR Model / %			Observed / %		
	Target	Lower Limit	Upper Limit	IR	NIR	MB
A	3.83	2.87	5.11	3.92 ± 0.23	3.85 ± 0.46	3.58 ± 0.07
B	3.23	2.41	4.33	2.70 ± 0.43	2.48 ± 0.79	2.81 ± 0.08
C	1.79	1.32	2.43	1.00 ± 0.15	1.56 ± 0.63	0.56 ± 0.06
D	2.01	1.50	2.71	1.52 ± 0.19	0.86 ± 0.13	1.06 ± 0.34
E	0.95	0.70	1.29	0.71 ± 0.14	0.83 ± 0.27	0.69 ± 0.08
F	1.11	0.81	1.51	1.02 ± 0.07	0.96 ± 0.20	1.50 ± 0.09
G	1.46	1.07	1.98	1.30 ± 0.14	1.54 ± 0.26	1.44 ± 0.06
H	2.69	1.97	3.69	3.02 ± 0.44	3.23 ± 0.39	3.24 ± 0.06
I	3.01	2.25	4.02	2.93 ± 0.30	2.70 ± 0.28	2.61 ± 0.13
J	1.87	1.39	2.51	1.53 ± 0.19	1.43 ± 0.11	1.42 ± 0.07
K	1.59	1.19	2.14	0.83 ± 0.14	0.92 ± 0.16	0.71 ± 0.14
L	2.35	1.76	3.15	1.86 ± 0.17	1.64 ± 0.22	2.54 ± 0.10
M	4.57	3.37	6.20	5.58 ± 0.56	4.49 ± 0.41	5.54 ± 0.09
N	4.77	3.55	6.42	4.64 ± 0.93	5.69 ± 0.43	4.48 ± 0.10
O	2.58	1.93	3.46	2.38 ± 0.35	2.28 ± 0.41	2.48 ± 0.06

Figure Captions

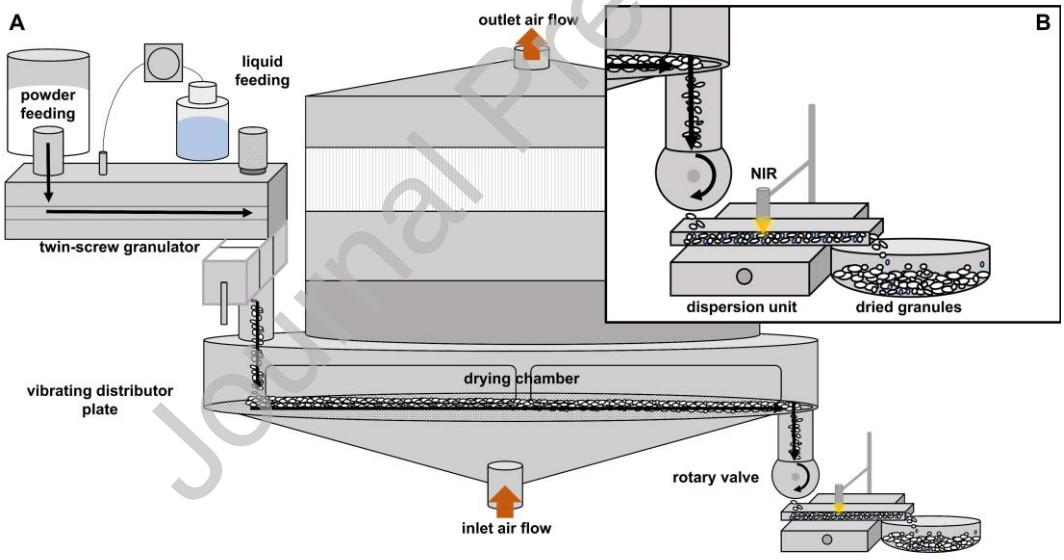

Figure 1. Experimental setup for LOD measurement via NIR spectroscopy.

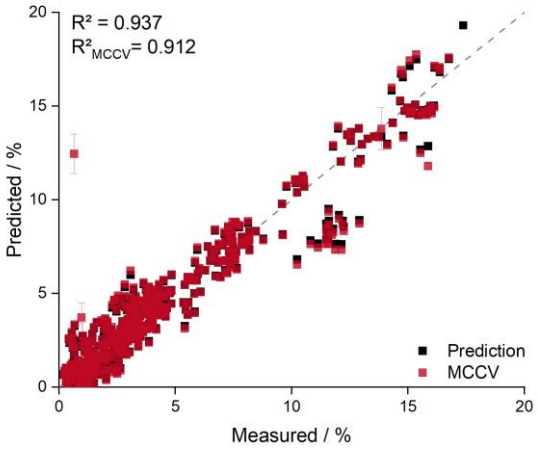

Figure 2. Calibration and cross-validation of NIR sensor with the offline LOD measurement via IR showing each individual LOD value.

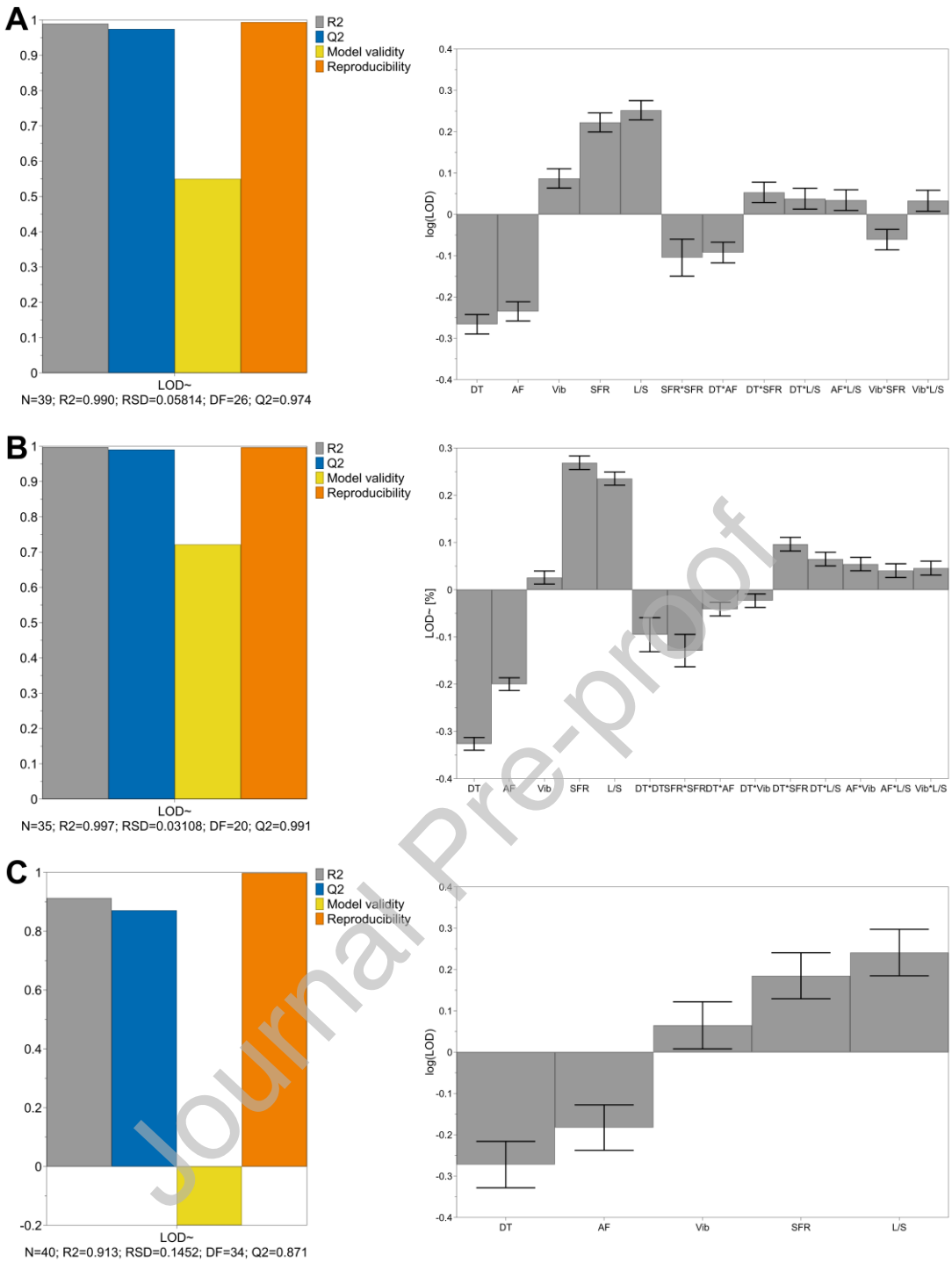

Figure 3. Summary of fit (left) and coefficient plot (right) for logarithmic LOD measured with standard method IR (A), NIR (B) and MB (C), mean coefficient ± 95 % confidence interval. The coefficient constants are 0.58 (IR), 0.64 (NIR) and 0.52 (MB).

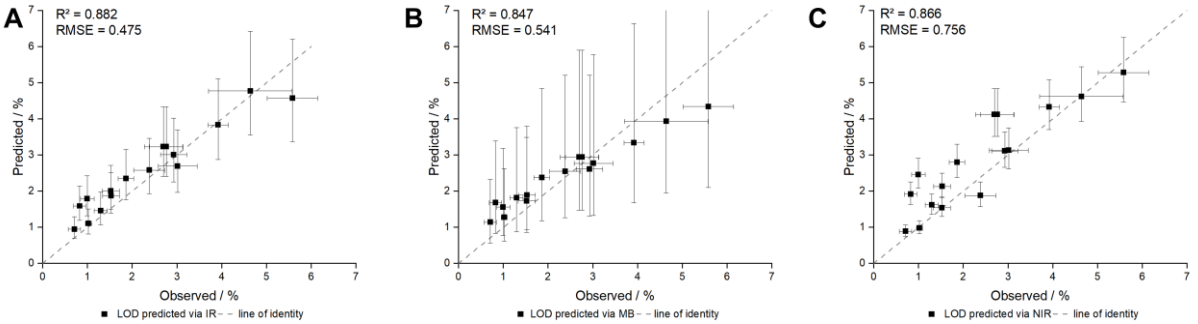

Figure 4. Verification of the LOD prediction models setup with LOD determination via IR (A), NIR (B) and MB (C). Predicted values ± 95 % prediction interval and observed is always the LOD via IR with n = 9, $\bar{x} \pm s$.

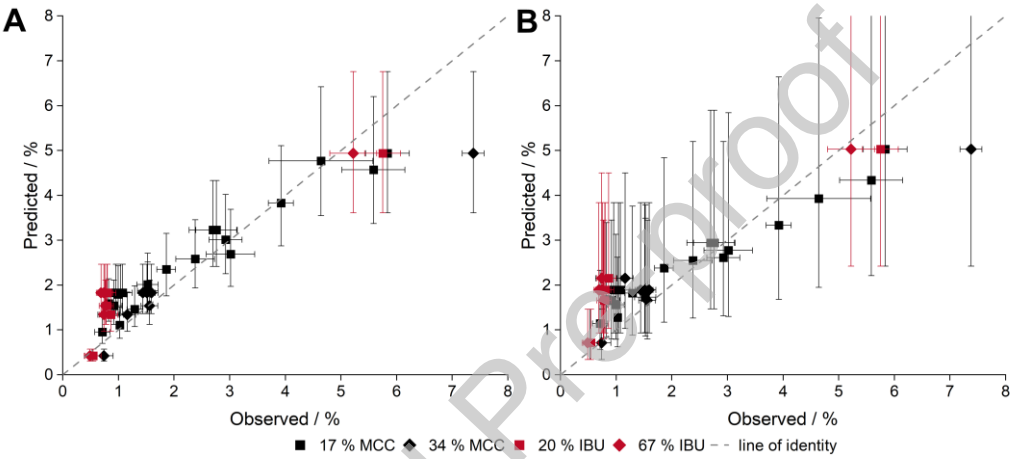

Figure 5. Verification of the LOD prediction models setup with LOD determination via IR (A) and MB (B) for different formulations. Predicted values ± 95 % prediction interval and observed is always the LOD via IR with n = 9, $\bar{x} \pm s$.

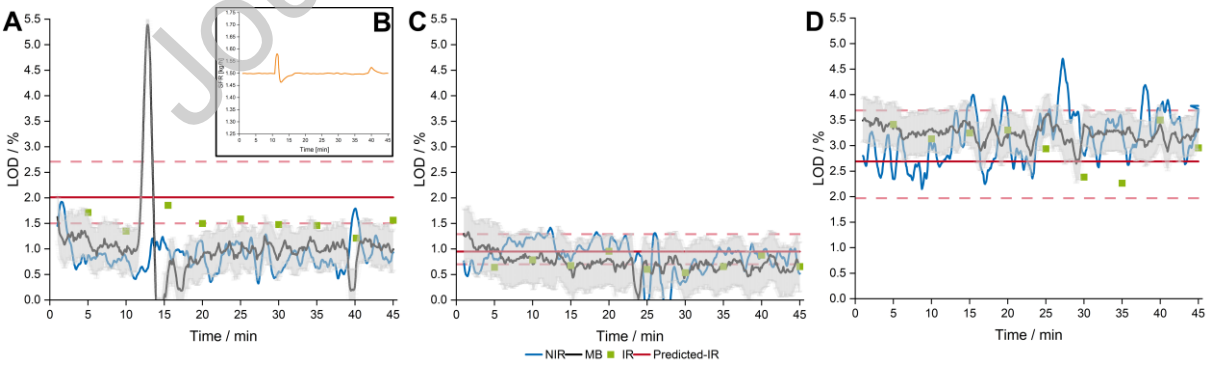

Figure 6. LOD predicted with MB as predicted ± uncertainty of the sensors, NIR and measured with IR. The red line depicts the predicted LOD using the IR model for runs D (A) with SFR (B), E(C) and H (D), while the red dotted lines show the upper and lower prediction limits with a 95 % prediction interval.

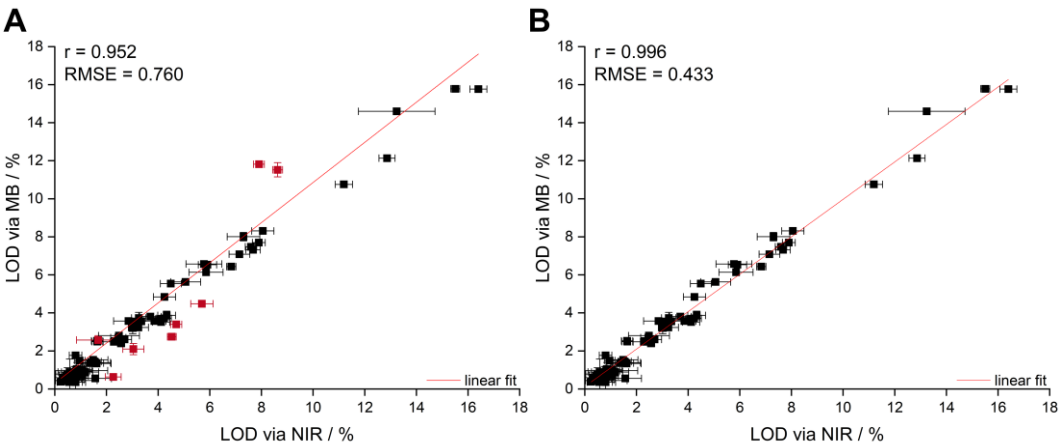

Figure 7. Correlation of LOD predicted via NIR and MB, n = 1350 timepoints (NIR) and n = 2700 timepoints (MB) for all runs (A) and after removing the red runs (B), $\bar{x} \pm s$.

Graphical Abstract

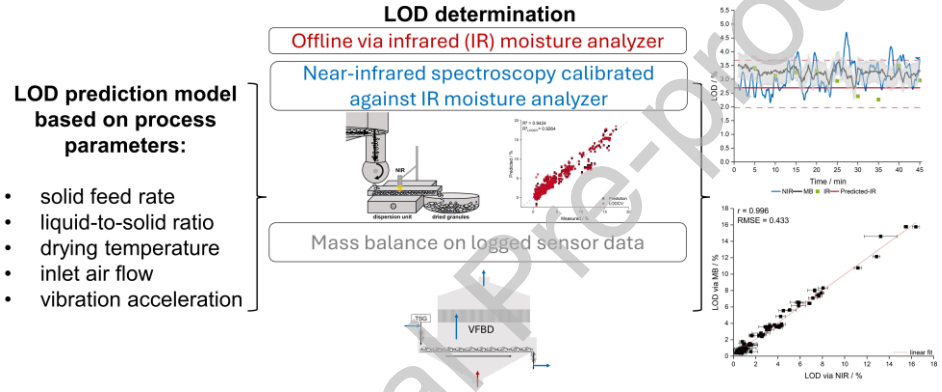

Declaration of interests

☒ The authors declare that they have no known competing financial interests or personal relationships that could have appeared to influence the work reported in this paper.

☐The authors declare the following financial interests/personal relationships which may be considered as potential competing interests: